FEBS Letters 582 (2008) 4169–4175

Effect of hyperoxidized guanine on DNA primer–template structures: Spiroiminodihydantoin leads to strand slippage

Dickson Fenn, Lai Man Chi, Sik Lok Lam*

Department of Chemistry, The Chinese University of Hong Kong, Shatin, New Territories, Hong Kong

Received 11 October 2008; revised 13 November 2008; accepted 17 November 2008

Available online 28 November 2008

Edited by Hans Eklund

Abstract **Oxidation of guanine in DNA can lead to mutagenic lesions such as 7-hydro-8-oxoguanine (oG). Upon further oxidation, a more mutagenic lesion, spirominodihydantoin (Sp), can occur. In this study, nuclear magnetic resonance (NMR) investigations were performed to determine the structural features of DNA primer–template models with 5′-GG, 5′-G(oG), 5′-G(Sp) and 5′-T(Sp) templates, that mimic the situation in which the downstream G of the template has been oxidized to oG or hyperoxidized to Sp. Our results show that misalignment occurs only in the 5′-G(Sp) and 5′-T(Sp) templates, providing structural insights into the observed differences in mutagenicity of Sp and oG during DNA replication.**

Keywords: NMR; DNA; Guanine; Spiroiminodihydantoin; Strand slippage

1. Introduction

Oxidative DNA damage is commonly caused by reactive oxygen species, and if not repaired, will lead to aging, cancers and neurodegenerative diseases [1]. Among the four DNA nucleobases, G has the lowest reduction potential, which makes it vulnerable to be oxidized to mainly 7-hydro-8-oxoguanine (oG) that has an even lower reduction potential [2]. oG can pair with C, A and G [3–5], and is considered to be responsible for G → T transversion and frameshift mutations [6]. oG is susceptible to further oxidation, resulting in a series of lesions including spiroiminodihydantoin (Sp) (Fig. 1A) [7]. Sp has been shown to be more mutagenic than oG and has two diastereomeric forms, namely Sp1 and Sp2. Their absolute configurations have been recently been determined [8]. They block replication, lead to G → C/T transversions and 1-base pair deletion [9–11].

Recent studies have revealed that Sp significantly lowers the stability of B-DNA [12] and prefers to position in the major groove [13]. The similarity of hydrogen bonding functionality of Sp in mimicking T [14] and the proclivity of incorporation of A against Sp [9] suggest Sp · A base pairing is favorable. Yet no experimental structural evidence has been obtained.

Despite the presence of lesions can slow or stall the action of polymerase, low fidelity DNA polymerases have shown the capability to accommodate misaligned primer–template in their loose active sites [15,16], and thus, DNA replication can continue and deletion error can occur. Recently, we have demonstrated that misalignment can occur at the replicating sites of primer–templates [17–19], yet the structural effect of Sp and oG lesions at these sites remains elusive.

In this study, we have performed nuclear magnetic resonance (NMR) investigations of primer–template models with a 5′-GX (where X = G, oG or Sp) (Fig. 1B) and 5′-T(Sp) templates (Fig. 1C). We found misalignment only occurred in 5′-G(Sp) and 5′-T(Sp), but not in 5′-GG and 5′-G(oG) templates, revealing Sp leads to strand slippage more easily than oG.

2. Materials and methods

2.1. Sample design

DNA samples were designed to form a hairpin with a 5′-GAA loop which connects the primer and template strands. Fig. 1B shows the three samples mimicking the situation in which a deoxycytidine triphosphate (dCTP) has just been incorporated opposite a 5′-GX template, whereas Fig. 1C shows a deoxyadenosine triphosphate (dATP) opposite a 5′-T(Sp) template. These samples were named as 5′-GG, 5′-G(oG), 5′-G(Sp) and 5′-T(Sp).

2.2. Sample preparation

DNA samples were synthesized using an ABI 394 DNA synthesizer and purified using polyacrylamide gel electrophoresis (PAGE) and diethylaminoethyl (DEAE) Sephacel column chromatography. To prepare 5′-G(Sp) and 5′-T(Sp), 5′-G(oG) and 5′-T(oG) samples were oxidized following the published protocol [9]. The final products were purified by high performance liquid chromatography (HPLC) (Appendix A, S1) and confirmed by matrix-assisted laser desorption ionization-time-of-flight mass spectrometry (MALDI-TOF MS) (Appendix A, S2). NMR samples were prepared by dissolving 0.50, 0.42, 0.85, 0.33 and 0.27 μmol of purified 5′-GG, 5′-G(oG), 5′-G(Sp), 5′-T(Sp1) and 5′-T(Sp2), respectively, into 500 μL of buffer solution containing 150 mM sodium chloride (NaCl), 10 mM sodium phosphate (NaPi) (pH 7.0), and 0.1 mM 2,2-dimethyl-2-silapentane-5-sulfonic acid (DSS).

*Corresponding author. Fax: +852 2603 5057.
E-mail address: lams@cuhk.edu.hk (S.L. Lam).

Abbreviations: NMR, nuclear magnetic resonance; oG, 7-hydro-8-oxoguanine; Sp, spiroiminodihydantoin; dCTP, deoxycytidine triphosphate; dATP, deoxyadenosine triphosphate; 1D, one-dimensional; 2D, two-dimensional; NOE, nuclear Overhauser effect; NOESY, nuclear Overhauser effect spectroscopy; DQF, double-quantum-filtered; COSY, correlation spectroscopy; TOCSY, total correlation spectroscopy; HSQC, heteronuclear single quantum coherence spectroscopy; UV, ultra-violet; DSS, 2,2-dimethyl-2-silapentane-5-sulfonic acid; WATERGATE, water suppression by gradient-tailored excitation; PAGE, polyacrylamide gel electrophoresis; DEAE, diethylaminoethyl; NaCl, sodium chloride; NaPi, sodium phosphate; HPLC, high performance liquid chromatography; MALDI, matrix-assisted laser desorption ionization; TOF, time-of-flight; MS, mass spectrometry

0014-5793/$34.00
doi:10.1016/j.febslet.2008.11.021

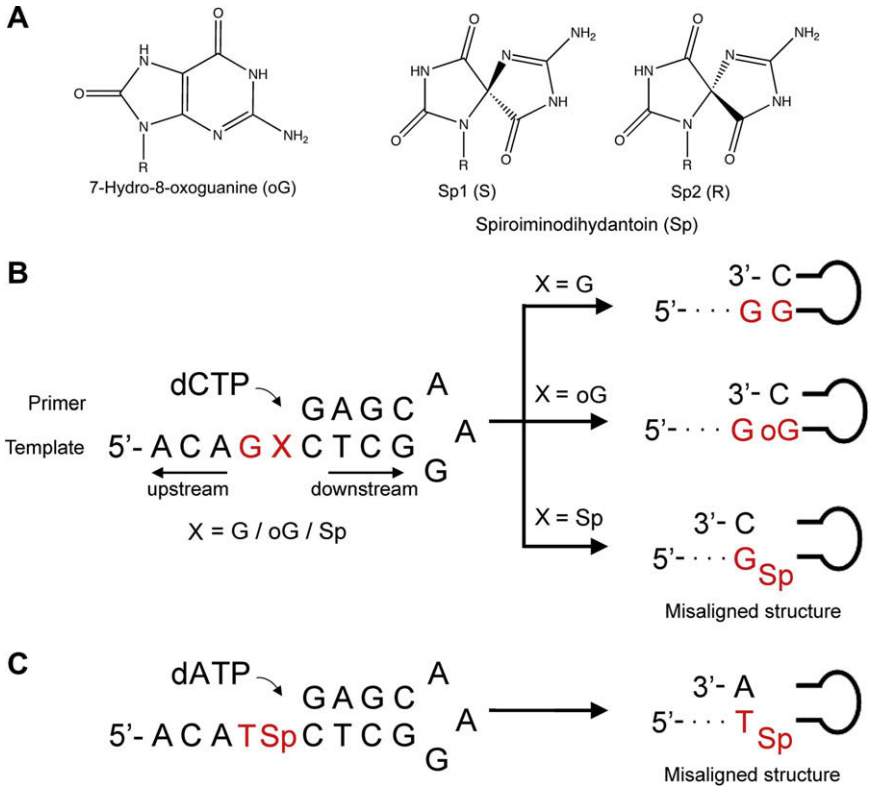

Fig. 1. (A) Chemical structures of oG and Sp, (B) design of primer–template models and outcomes of this study, and (C) misalignment was also observed in 5′-T(Sp) template.

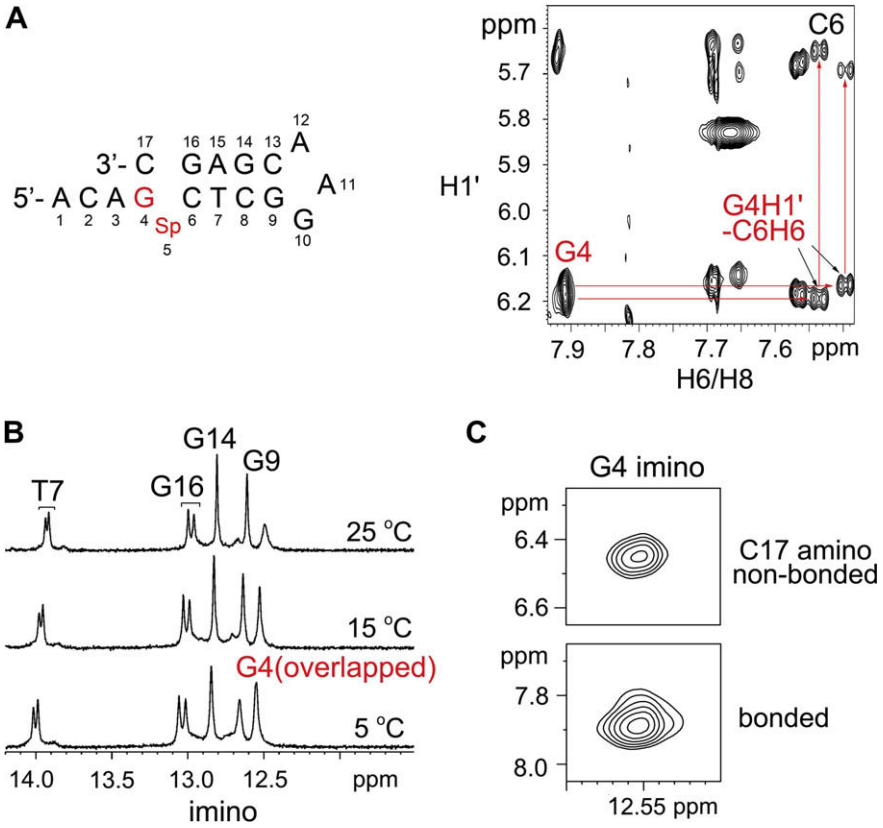

Fig. 2. (A) Unusual G4 H1′–C6 H6 NOEs in 5′-G(Sp) at 25 °C. The presence of (B) G4 imino signal, and (C) G4 imino–C17 amino NOEs at 5 °C, indicates C17 · G4 base pair.

2.3. NMR study

NMR experiments were performed using Bruker 500 MHz spectrometers. Labile protons were studied using water suppression by gradient-tailored excitation (WATERGATE) [20], and jump-return [21] methods on samples in 90% H_2O/10% D_2O. For studying non-labile protons, the solvent was exchanged with a 100% D_2O. Two-dimensional (2D) nuclear Overhauser effect spectroscopy (NOESY) experiments with 4 K × 512 data size were performed at 100, 200 and 300 ms mixing times. To minimize spectral overlap, some of the experiments were repeated at various temperatures. 2D total correlation spectroscopy (TOCSY) at 75 ms mixing time and double-quantum-filtered correlation spectroscopy (DQF-COSY) experiments were conducted. For DQF-COSY, a sine window function was used and the data were zero-filled to 16 K × 16 K for measuring $^3J_{H1'H2'}$ and $^3J_{H1'H2''}$ and calculating the percentage of S-state (%S) [22].

^1H–^{31}P heteronuclear single quantum coherence spectroscopy (HSQC) experiments with 4 K × 256 data size were also conducted with ^1H and ^{31}P spectral widths of 11 and 3 ppm, respectively. ^{31}P chemical shifts were indirectly referenced to DSS [23]. ^1H–^{31}P COSY experiments with 4 K × 160 data size and a Gaussian inversion pulse centered at the H3′ region were also performed. The ^{31}P dimension was linearly predicted to 256 data points and zero-filled to 16 K points for measuring $^3J_{H3'P}$ and calculating the percentage of B_I conformation (%B_I) [24].

2.4. Thermodynamics study

Ultra-violet (UV) absorbance data were measured versus temperatures from 25 to 90 °C at a heating rate of 0.8 °C/min using a HP 8453 Diode-Array UV spectrophotometer. The DNA sample concentrations were kept at 3.2 μM. Thermodynamic parameters were determined from the melting curves using MELTWIN 3.5.

3. Results and discussion

NMR spectroscopic investigations focusing on one-dimensional (1D) imino proton and 2D NOESY analyses were performed. Sequential assignments were made by studying the 2D NOESY and WATERGATE-NOESY spectra (Appendix A, S3–S7). H1′, H2′ and H2″ assignments were shown in Appendix A, S8 and ^{31}P assignments in Appendix, S9. In addition, the chemical shifts of both labile and non-labile protons were tabulated in Appendix A, S10–S14.

3.1. Preparation of 5′-G(Sp) and 5′-T(Sp)

The presence of Sp1 and Sp2 complicated the sample preparative work in this study. Based on HPLC results, the overall product yield for 5′-G(Sp) and 5′-T(Sp) was ~30%. We attempted to separate the two isomers of 5′-G(Sp), 5′-T(Sp) and some other sequences containing Sp1 and Sp2 (Appendix A, S1). Our results reveal that the separation depends on the sequence context, as observed in other studies [11,25]. Although the separation of 5′-G(Sp) isomers was not successful, one set of resonance signals was observed from each isomer (Appendix A, S3).

3.2. Misalignment occurs in 5′-G(Sp), but not in 5′-GG and 5′-G(oG) Templates

When dCTP was incorporated opposite the 5′-G(Sp) template, instead of interacting with Sp, the dCTP paired with the upstream G, resulting in a misaligned structure with a

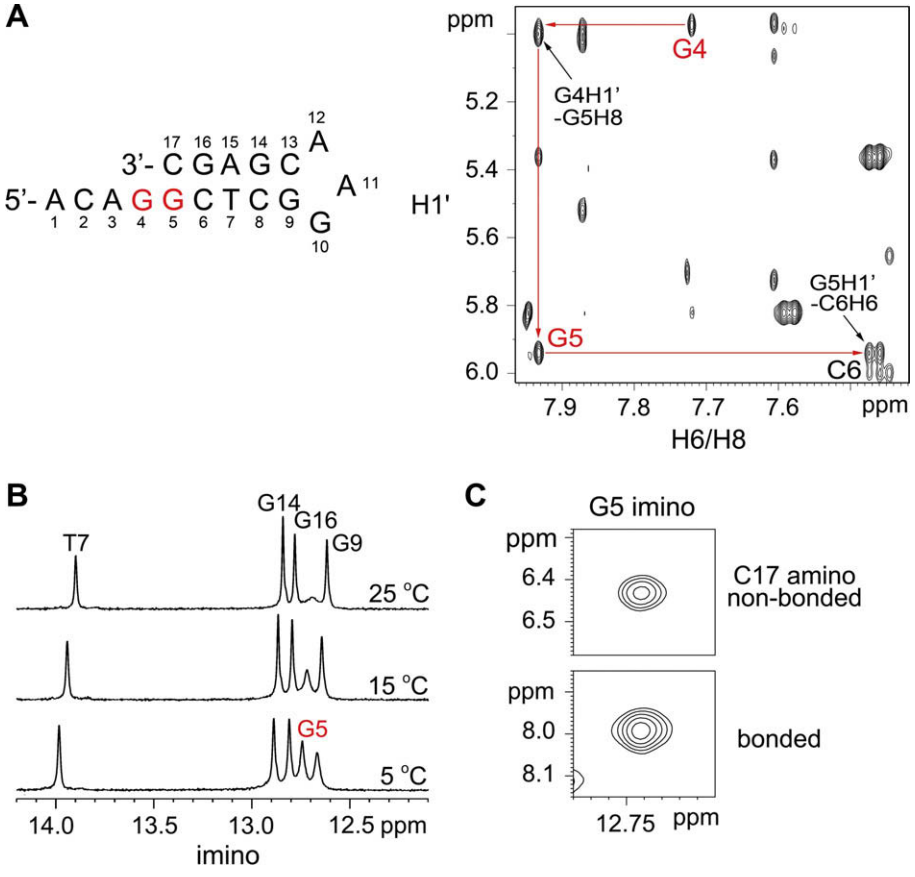

Fig. 3. (A) The sequential G4–G5 and G5–C6 NOEs at 25 °C suggest no misalignment. The presence of (B) G5 imino signal, and (C) G5 imino–C17 amino NOEs at 5 °C, indicates C17 · G5 base pair.

Sp-bulge and a terminal C17 · G4 Watson–Crick base pair. This was evidenced by the unusual G4 H1′–C6 H6 nuclear Overhauser effect (NOE) crosspeak, indicating G4 and C6 were close in space (Fig. 2A). Owing to the presence of Sp1 and Sp2 diastereomers in 5′-G(Sp), two G4 H1′–C6 H6 NOEs were observed. In addition, the presence of two G4 imino signals that were overlapped (Fig. 2B) and two sets of NOEs between the G4 imino and overlapped C17 amino protons (Fig. 2C) indicate the formation of a C17 · G4 Watson–Crick base pair, confirming the misaligned structures with a Sp-bulge and a closing C · G Watson–Crick base pair. This structural finding is similar to our previous observations on misaligned structures with a T-bulge [17,18] or C-bulge [19] in pyrimidine templates.

On the other hand, when dCTP was incorporated opposite the 5′-GG and 5′-G(oG) templates, no misaligned structure was formed at neither replicating sites. Fig. 3A shows the sequential G4 H1′–G5 H8 and G5 H1′–C6 H6 NOEs of 5′-GG, suggesting no misaligned structure was formed at the replicating site. This was further supported by the absence of an unusual G4 H1′–C6 H6 NOE. Based on the sequential resonance assignments, the labile G5 imino and C17 amino protons of 5′-GG were identified in the WATERGATE-NOESY (Appendix A, S4). A C17 · G5 Watson–Crick base pair was formed as evidenced by the G5 imino signal at ~12.75 ppm (Fig. 3B) and an NOE between G5 imino and C17 amino protons (Fig. 3C) at 5 °C. This newly formed base pair was fairly stable as G5 imino signal remained observable at 15 and 25 °C (Fig. 3B).

For 5′-G(oG) template, two conformers were observed in the 2D NOESY fingerprint region (Appendix A, S5), of which from the peak integrals of A3 H8 and G4 H8 in the 1D proton spectra, the major conformer was estimated to have a 70–80% population. For the major conformer, a sequential oG5 H1′–C6 H6 NOE was observed (Fig. 4A). It was overlapped with the G16 H1′–G16 H8 NOE at 25 °C, but better resolved at 5 °C. Moreover, a terminal C17 · oG5 Watson–Crick base pair was formed as evidenced by an oG5 imino signal at ~12.9 ppm (Fig. 4B) and an NOE with C17 amino proton in the WATERGATE-NOESY spectrum at 5 °C (Fig. 4C). The result agrees with a previous NMR finding that C · oG base pair adopts the Watson–Crick pairing mode in the stem region of a double-helix [3]. For the minor conformer, it probably adopts a homoduplex structure. This is supported by an increase in their peak intensities at higher salt and DNA concentrations, similar chemical shifts and broader line-widths when compared to those of the major conformer (Appendix A, S5C).

For the primer–template structures of 5′-G(Sp), 5′-GG and 5′-G(oG), all bases in the double-helical stem region adopt an *anti* glycosidic orientation with respect to their sugar rings as

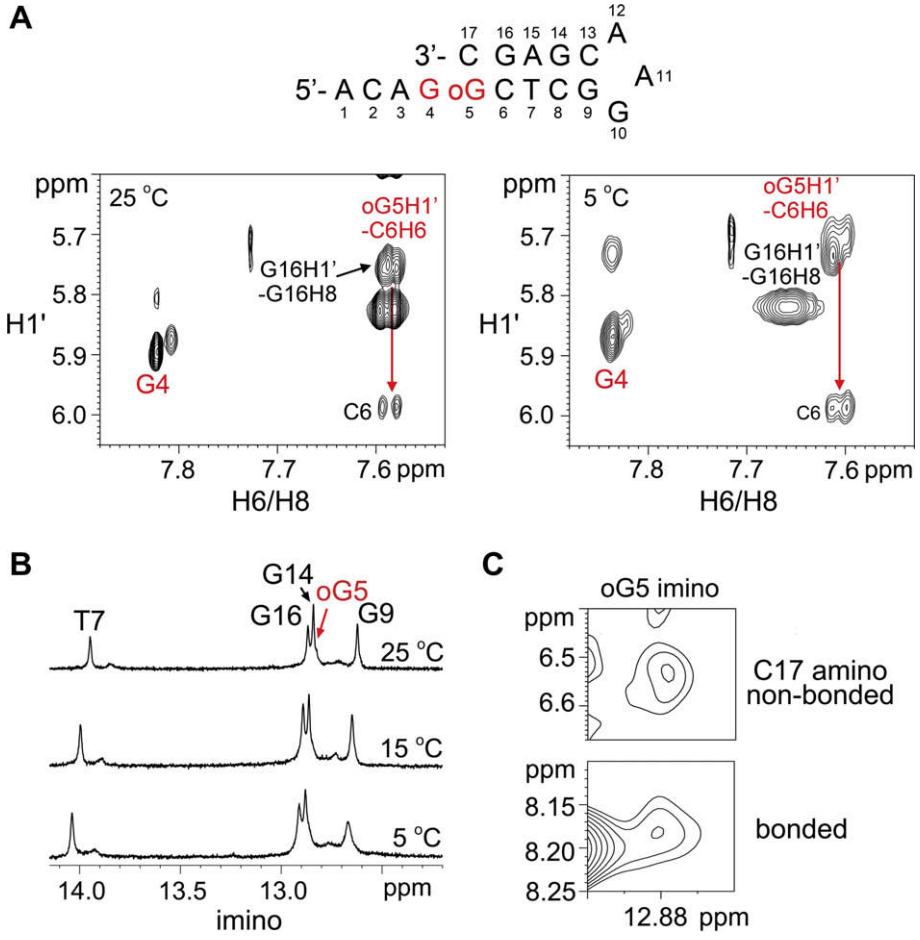

Fig. 4. (A) Sequential oG5 H1′–C6 H6 NOE, partially overlapped with G16 H1′–G16 H8 NOE, was observed at 25 °C and better resolved at 5 °C. The presence of (B) oG5 imino signal, and (C) imino–C17 amino proton NOEs at 5 °C, indicates C17 · oG5 base pair.

evidenced by their intranucleotide H8/H6–H1′ NOEs with intensities weaker than that of cytosine H5–H6 NOEs (Appendix A, S3–S5) [26]. However, for the sugar puckers of G4 and C6 of 5′-G(Sp), their %S values were reduced by at least 20% when compared to those of 5′-GG and 5′-G(oG) (Appendix A, S15). For the backbone conformations near the replicating sites, the $\%B_I$ values of 5′-GG, 5′-G(oG) and 5′-G(Sp) were similar (Appendix A, S16).

Unlike a severe destabilizing effect of Sp observed in regular DNA duplexes [12], such effect was less pronounced in 5′-G(Sp) (Appendix A, S17). This is probably because Sp is bulged out which allows favorable stacking interaction between the terminal C17 · G4 Watson–Crick base pair and the penultimate G16 · C6 base pair in the misaligned structure. The formation of the misaligned structure in 5′-G(Sp) suggests that the stabilization gained by the formation of the terminal C · G Watson–Crick base pair outweighs the destabilizing effect of the Sp-bulge. This was supported by the observed similar thermodynamic stabilities between 5′-G(oG) and 5′-G(Sp) (Appendix A, S17).

3.3. Misalignment also occurs upon incorporation of a dATP opposite a 5′-T(Sp) template

Besides the study on 5′-G(Sp), we have also investigated the situation when dATP was incorporated opposite a 5′-T(Sp) template since Sp · A base pairing has been suggested to be possible [9,14]. Our results show that instead of interacting with Sp, the dATP paired with the upstream T, leading to a misaligned structure with a Sp-bulge and a terminal A17 · T4 Watson–Crick base pair. This was evidenced by the unusual T4 H1′–C6 H6 NOE in both the Sp1 and Sp2 isomers (Fig. 5A). In 5′-G(Sp), a G4 imino–C17 amino NOE was observed at 5 °C (Fig. 2C), which further supports the misaligned structure. However, due to the faster imino exchange rate of terminal A17 · T4 Watson–Crick base pair in 5′-T(Sp), T4 imino–A17 H2 NOE was not observed even at 0 °C (Appendix A, S6B and S7B). Nevertheless, an additional imino signal appeared in the Watson–Crick base pair imino region at lower temperatures (Fig. 5B), suggesting the formation of A17 · T4 base pair. All bases in the double-helical stem region of 5′-T(Sp) adopt an *anti* glycosidic orientation (Appendix A, S6 and S7). For the sugar pucker, all nucleotides behave similarly to those observed in 5′-G(Sp) (Appendix A, S15). The %S values of T4 and C6 were also reduced by at least 20% when compared to those of the primer–templates without misalignment. The $\%B_I$ values were also similar to all other primer–templates (Appendix A, S16). These suggest that the formation of Sp-bulge was accompanied predominantly by the change of the sugar puckers flanking the Sp-bulge. The major structural difference between the Sp1 and Sp2 diastereomers of 5′-G(Sp)

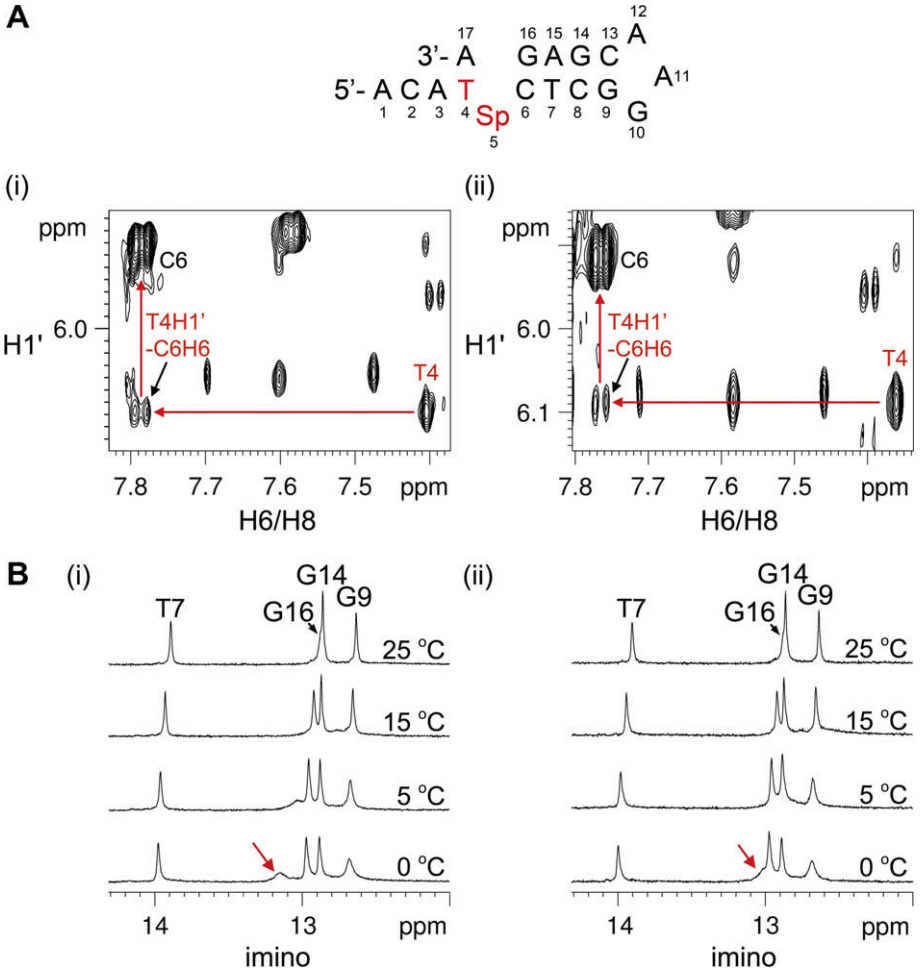

Fig. 5. (A) Unusual T4 H1′–C6 H6 NOEs in the (i) Sp1, and (ii) Sp2 isomers of 5′-T(Sp) at 25 °C. (B) Additional imino signal (indicated by red arrow) in the jump-return spectra at lower temperatures in both the (i) Sp1 and (ii) Sp2 isomers suggests A17 · T4 base pair.

and 5′-T(Sp) were found in the sugar puckers of the Sp-bulges (Appendix A, S15). The perpendicular arrangement of two rings in Sp brings about diastereomeric specificity [27,28], which is probably the reason for the observed differences in their %S values.

The thermodynamic stability of the misaligned 5′-T(Sp) was found to be ~0.8 kcal/mol lower than that of 5′-G(Sp) (Appendix A, S17), probably due to the differences in stabilities of the terminal A · T and C · G base pairs and the stacking energies with their flanking base pairs. In addition, the two rings of Sp are perpendicular to each other which disturb base stacking [13], the presence of the Sp · C or Sp · A base pair in the mismatched conformer is less favorable and thus the misaligned structure is preferred.

In short, our results show that strand slippage occurs in both the 5′-G(Sp) and 5′-T(Sp) templates upon incorporation of a dCTP and dATP, respectively, suggesting a possible pathway for the occurrence of 1-base pair deletion during DNA replication and providing insights into the observed differences in mutagenicity of Sp and oG. Yet, further structural investigations with DNA polymerases are needed since individual DNA polymerases are likely to interact with primer–template differently and the extent to which these structures occur in DNA polymerases may also depend upon the specific polymerase in question.

Acknowledgment: The work described in this paper was fully supported by a grant from the Research Grants Council of the Hong Kong Special Administrative Region (Project No. CUHK400704).

Appendix A. Supplementary data

Figures showing HPLC chromatograms, mass spectra, NMR sequential assignments, NOESY, DQF-COSY and $^{1}H-^{31}P$ HSQC spectra, tables summarizing proton chemical shift, %S and $\%B_I$ and thermodynamics of the primer−templates. Supplementary data associated with this article can be found, in the online version, at doi:10.1016/j.febslet.2008.11.021.

References

[1] Finkel, T. and Holbrook, N.J. (2000) Oxidants, oxidative stress and the biology of ageing. Nature 408, 239–247.
[2] Steenken, S., Jovanovic, S.V., Bietti, M. and Bernhard, K. (2000) The trap depth (in DNA) of 8-oxo-7,8-dihydro-2′-deoxyguanosine as derived from electron-transfer equilibria in aqueous solution. J. Am. Chem. Soc. 122, 2373–2374.
[3] Oda, Y., Uesugi, S., Ikehara, M., Nishimura, S., Kawase, Y., Ishikawa, H., Inoue, H. and Ohtsuka, E. (1991) NMR studies of a DNA containing 8-hydroxydeoxyguanosine. Nucl. Acid Res. 19, 1407–1412.
[4] Kouchakdjian, M., Bodepudi, V., Shibutani, S., Eisenberg, M., Johnson, F., Grollman, A.P. and Patel, D.J. (1991) NMR structural studies of the ionizing radiation adduct 7-hydro-8-oxodeoxyguanosine (8-oxo-7H-dG) opposite deoxyadenosine in a DNA duplex. 8-Oxo-7H-dG(syn).dA(anti) alignment at lesion site. Biochemistry 30, 1403–1412.
[5] Thiviyanathan, V., Somasunderam, A., Hazra, T.K., Mitra, S. and Gorenstein, D.G. (2003) Solution structure of a DNA duplex containing 8-hydroxy-2′-deoxyguanosine opposite deoxyguanosine. J. Mol. Biol. 325, 433–442.
[6] Neeley, W.L. and Essigmann, J.M. (2006) Mechanisms of formation, genotoxicity, and mutation of guanine oxidation products. Chem. Res. Toxicol. 19, 491–505.
[7] Adam, W., Arnold, M.A., Gruene, M., Nau, W.M., Pischel, U. and Saha-Moeller, C.R. (2002) Spiroiminodihydantoin is a major product in the photooxidation of 2′-deoxyguanosine by the triplet states and oxyl radicals generated from hydroxyacetophenone photolysis and dioxetane thermolysis. Org. Lett. 4, 537–540.
[8] Durandin, A., Jia, L., Crean, C., Kolbanovskiy, A., Ding, S., Shafirovich, V., Broyde, S. and Geacintov, N.E. (2006) Assignment of absolute configurations of the enantiomeric spiroiminodihydantoin nucleobases by experimental and computational optical rotatory dispersion methods. Chem. Res. Toxicol. 19, 908–913.
[9] Henderson, P.T., Delaney, J.C., Muller, J.G., Neeley, W.L., Tannenbaum, S.R., Burrows, C.J. and Essigmann, J.M. (2003) The hydantoin lesions formed from oxidation of 7,8-dihydro-8-oxoguanine are potent sources of replication errors in vivo. Biochemistry 42, 9257–9262.
[10] Kino, K. and Sugiyama, H. (2005) UVR-induced G–C to C–G transversions from oxidative DNA damage. Mutat. Res. 571, 33–42.
[11] Neeley, W.L., Delaney, S., Alekseyev, Y.O., Jarosz, D.F., Delaney, J.C., Walker, G.C. and Essigmann, J.M. (2007) DNA polymerase V allows bypass of toxic guanine oxidation products in vivo. J. Biol. Chem. 282, 12741–12748.
[12] Chinyengetere, F. and Jamieson, E.R. (2008) Impact of the oxidized guanine lesion spiroiminodihydantoin on the conformation and thermodynamic stability of a 15-mer DNA duplex. Biochemistry 47, 2584–2591.
[13] Jia, L., Shafirovich, V., Shapiro, R., Geacintov Nicholas, E. and Broyde, S. (2005) Structural and thermodynamic features of spiroiminodihydantoin damaged DNA duplexes. Biochemistry 44, 13342–13353.
[14] David, S.S., O'Shea, V.L. and Kundu, S. (2007) Base-excision repair of oxidative DNA damage. Nature 447, 941.
[15] Ling, H., Boudsocq, F., Woodgate, R. and Yang, W. (2001) Crystal structure of a Y-family DNA polymerase in action: a mechanism for error-prone and lesion-bypass replication. Cell 107, 91–102.
[16] Garcia-Diaz, M., Bebenek, K., Krahn, J.M., Pedersen, L.C. and Kunkel, T.A. (2006) Structural analysis of strand misalignment during DNA synthesis by a human DNA polymerase. Cell 124, 331–342.
[17] Chi, L.M. and Lam, S.L. (2006) NMR investigation of DNA primer–template models: structural insights into dislocation mutagenesis in DNA replication. FEBS Lett. 580, 6496–6500.
[18] Chi, L.M. and Lam, S.L. (2007) NMR investigation of primer–template models: structural effect of sequence downstream of a thymine template on mutagenesis in DNA replication. Biochemistry 46, 9292–9300.
[19] Chi, L.M. and Lam, S.L. (2008) Nuclear magnetic resonance investigation of primer–template models: formation of a pyrimidine bulge upon misincorporation. Biochemistry 47, 4469–4476.
[20] Sklenar, V., Piotto, M., Leppik, R. and Saudek, V. (1993) Gradient-tailored water suppression for $^{1}H-^{15}N$ HSQC experiments optimized to retain full sensitivity. J. Mag. Reson. Ser. A 102, 241–245.
[21] Plateau, P. and Gueron, M. (1982) Exchangeable proton NMR without base-line distortion, using new strong-pulse sequences. J. Am. Chem. Soc. 104, 7310–7311.
[22] van Wijk, J., Huckriede, B.D., Ippel, J.H. and Altona, C. (1992) Furanose sugar conformations in DNA from NMR coupling-constants. Meth. Enzymol. 211, 286–306.
[23] Markley, J.L., Bax, A., Arata, Y., Hilbers, C.W., Kaptein, R., Sykes, B.D., Wright, P.E. and Wuthrich, K. (1998) Recommendations for the presentation of NMR structures of proteins and nucleic acids. Pure Appl. Chem. 70, 117–142.
[24] Gorenstein, D.G. (1994) Conformation and dynamics of DNA and protein–DNA complexes by P-31 NMR. Chem. Rev. 94, 1315–1338.
[25] Kornyushyna, O., Berges, A.M., Muller, J.G. and Burrows, C.J. (2002) In vitro nucleotide misinsertion opposite the oxidized guanosine lesions spiroiminodihydantoin and guanidinohydantoin and DNA synthesis past the lesions using Escherichia coli

DNA polymerase I (Klenow fragment). Biochemistry 41, 15304–15314.
[26] Wüthrich, K. (1986) NMR of Proteins and Nucleic Acids, Wiley, New York.
[27] Jia, L., Shafirovich, V., Geacintov Nicholas, E. and Broyde, S. (2007) Lesion specificity in the base excision repair enzyme hNeil1: modeling and dynamics studies. Biochemistry 46, 5305–5314.
[28] Krishnamurthy, N., Zhao, X., Burrows, C.J. and David, S.S. (2008) Superior removal of hydantoin lesions relative to other oxidized bases by the human DNA glycosylase hNEIL1. Biochemistry 47, 7137–7146.